Title:	**Wind Load on Arena Roofs Using Aerodynamic Models**
Authors:	Daryl W. Boggs, Cermak Peterka Petersen (CPP), Inc. Jon A. Peterka, Cermak Peterka Petersen (CPP), Inc.
Subject:	Wind Engineering
Keyword:	Wind
Publication Date:	1993
Original Publication:	Structures Congress Irvine CA 1993
Paper Type:	1. **Book chapter/Part chapter** 2. Journal paper 3. Conference proceeding 4. Unpublished conference paper 5. Magazine article 6. Unpublished

Structural Engineering in Natural Hazards Mitigation, Vol. 1 (Proceedings of papers presented at the Structures Congress '93, Irvine, CA), ed. A.H-S. Ang and R. Villaverde, ASCE, 1993.

WIND LOADS ON ARENA ROOFS USING AERODYNAMIC MODELS

Daryl W. Boggs[1] and Jon A. Peterka[2]

According to the ASCE 7-88 standard and most building codes, frame wind loads on typical arena roofs are static and uniform. Only if the structure's natural frequency is less than 1 Hz is the dynamic response addressed; even then ASCE 7-88 simply calls for a multiplicative gust factor to be determined through "rational analysis."

Real wind loads on low-profile long-span roofs are likely to be neither uniformly distributed nor statically applied, as illustrated by the flow visualization in Fig. 1. The effective load on a major structural member, such as Truss A in Arena 1, Fig. 2, is represented by a temporal and spatial average of the pressure fluctuations over its tributary area. Power spectra of fluctuations measured at points 1, 2, and 3, along with their instantaneous average, are shown in Fig. 3. The peaks in the individual spectra at a frequency of 1-2 Hz indicate harmonic vortex excitation, existing at all three points, but having somewhat different characters. This is consistent with Fig. 1. The power spectrum of the average does not show this peak, due to phase differences and/or lack of correlation. The predicted dynamic response of the roof structure will be highly dependent on the natural frequencies and tributary areas of its structural members, according to how many pressure signals (and their separation distance) can be averaged together and the shape of the resulting load spectrum; that is, the amount of energy available for resonant excitation at the member's natural frequency.

This is the concept behind an aerodynamic wind-tunnel model used to predict dynamic response to wind excitation: the generalized load in a particular natural mode of vibration is measured, and analytically combined with dynamic properties of the structure (mass, stiffness, and damping) to compute the response. Results are expressed as static-equivalent loads by which the structure can be designed using classic static analysis. This paper illustrates the application to typical arena structures which have been investigated in the authors' wind tunnel laboratory.

Consider a 1-D member having damping ratio ζ, natural frequency f_0, mode shape $\phi(x)$, and generalized mass m^* within a particular mode of interest, acted upon by load intensity $w(x,t)$. In a wind-tunnel model the pressure is sampled at discrete points i, each associated with a tributary area a_i. The generalized load of this mode is

---

[1]Sr. Project Engineer, Cermak Peterka Petersen, Inc, 1415 Blue Spruce Drive, Ft. Collins, CO 80524

[2]Vice President, Cermak Peterka Petersen, Inc.

$$P^* = \int_0^L w(x,t)\phi(x)\,dx \approx \sum_{i=1}^{N} p_i(t) a_i \phi_i \tag{1}$$

The mean square generalized response of the mode can then be computed as

$$\tilde{\mathbf{P}}^{*2} = \int_0^\infty S_{P*}(f)\left|H(f)\right|^2 df \approx \frac{\pi}{4\zeta} f_0 S_{P*}(f_0) + \tilde{P}^{*2} \tag{2}$$

where $\left|H(f)\right|^2 = 1/\{[1-(f/f_0)^2]^2 + (2\zeta f/f_0)^2\}$ is the mode's mechanical admittance, and $S_{P*}(f)$ is the mean square spectral density (or *PSD*) of the generalized load. The first term on the right side of Eq. (2) represents the resonant response $\tilde{R}^2$, while the second term—essentially the directly applied wind gusts—represents the background response $\tilde{B}^2$. Peak static-equivalent loads are extracted from the mean square generalized response. For example, if the member is modeled as having discrete nodes j, the static-equivalent peak dynamic load at any node is given by

$$\hat{\mathbf{P}}_j = g_p \tilde{\mathbf{P}}_j = g_p \frac{m_j \phi_j}{m^*} \tilde{\mathbf{P}}^* \tag{3}$$

where g_p is a peak factor, evaluated analytically and generally ranging from 3 to 4.

This procedure is illustrated on Fig. 3 for the case of $f_0 = 2.3$ Hz and $\zeta = 0.01$. The rms background load $\tilde{B} = 0.42$, significantly less than the pressure at point 1 but greater than at point 3; the rms resonant response is $\tilde{R} = 0.89$; the rms generalized response is $\tilde{\mathbf{P}}^* = 0.98$, even higher than the pressure at an individual point. The dynamic amplification factor is $\tilde{\mathbf{P}}^* / \tilde{B} = 2.3$. Table 1 gives results obtained for members *A*, *D* in Arena 1, using only the fundamental mode of vibration. Resulting peak loads are simplified to the form of a mid-span pressure, including a measured mean pressure, and compared to the loads which would be computed using ASCE 7-88. These results show that the actual loads can be significantly less than or greater than conventional standards would indicate, and may even be in the opposite direction. The loading distribution adds further complexity, as illustrated in Fig. 4. By considering the actual (measured) distribution of mean pressure, and possibly including the response in higher modes, a significantly unbalanced load can result. Also, a small downward load may be more critical than a larger upward load, depending on the dead load, design live load and other loads, and the significance of stress reversal in bottom chord members. Evidently, the members most in need of investigation, and their critical loading condition, may be very difficult to predict.

We now turn our attention to certain instrumentation difficulties routinely encountered in the wind tunnel tests. Foremost among these is that of frequency response. Table 2 summarizes the natural frequencies of major structural members in the arenas from Fig. 2. The fundamental-mode f_0 ranges from 0.7 to 2.45 Hz; second mode f_0 ranges to 6.59 Hz. At typical model scales (1:200) and test wind speeds (50 fps) the model frequencies are 50 to 70 times higher. According to Eq. (2) the instrument system must be capable of measuring *at least* up to f_0. This requires a bandwidth of typically 150 to 250 Hz; occasionally higher. While a bandwidth of 250 Hz is generally recommended for routine measurement of peak pressures in a conventional model used for cladding design, this is needed only to obtain accuracy within a few percent since the major frequencies of interest are on the order of 0.1 to 2 Hz full scale (as indicated by individual tap data in Fig. 3) or 5 to 100 Hz model scale; a measurement error of, say, 50 percent at 200 Hz is not serious. For use in an aerodynamic model where the structure's scaled natural frequency is 250 Hz, however, such a measurement error is intolerable.

Figure 5 shows the PSD of the generalized loads in modes 1 and 2 for Member C, Arena 2. These were synthesized using Eq. (1) from pressures measured at several locations along the member shown in Fig. 2, using very short tube lengths to optimize frequency response. The time series pressure data were processed, using a digital filter corresponding to the inverse of an appropriate pressure tube admittance function, to produce PSD's valid up to more than 600 Hz. The second-mode response is observed to be several times less than that of the first mode. It is of interest to note that at a wind direction of 180 degrees the second-mode response will always be less than the first, since the natural frequency of mode 2 is always higher than in mode 1. At 247.5 degrees, however, the second-mode response could be higher if its natural frequency were between 40 and 200 Hz (model scale; about 0.5 to 3 Hz full scale). This situation can often occur if the wind direction is not normal to the structural member.

A second difficulty encountered is obtaining adequate spatial resolution of the pressure gradients, in combination with appropriate area and modal weighting factors, for use in Eq. (1). The problem here is that all of the pressure time series used must be measured simultaneously. The examples considered so far featured simple members having one-dimensional mode shapes supporting a roof of simple contour, so that a few pressure taps is adequate. The perimeter girder *P* in Arena 3 has a 1-D mode shape; however, contributing pressures derive from both the lower roof to the north and an adjacent portion of the triangular segment of the main roof, due to north-south beams framing between trusses *P* and *X*. The 8 taps indicated in Fig. 2 illustrate the difficulty of defining the generalized load using a measurement system with limited channels/pressure transducers. With a limited channel capacity, spatial resolution can often be increased by means of pneumatic averaging, as indicated by the taps on Member A on Arena 2. In this case, transducer/ch. 1 measures the average pressure p_1 of 6 taps, etc. The tap locations and spacing within each group must be carefully planned so that the resulting pressure represents an appropriate weighted area average. Another disadvantage of pneumatic averaging is that the manifold and tube lengths can complicate and degrade the system frequency response. The cross truss *X* in Arena 3 demonstrates a further source of spatial resolution complexity; this member has 2-D mode shapes which involve the entire high roof. A large number of taps is required to accurately define the generalized loads, especially in the higher modes.

Finally there is the matter of convenience. Even for a simple roof geometry and 1-D mode shapes which can be adequately covered by a few tap locations, it may be difficult if not impossible to predict which areas should be investigated, in order to limit the number of taps installed and the wind-tunnel run time. In fact, the structural scheme may not even have been completely defined at the time of model testing. A large number of pressure taps—perhaps 100 or more—is usually installed in the model roof to measure peak cladding pressures, however these are not likely to be adequately spaced for modal and area weighting definition if the generalized load is to be synthesized from only a few local pressure or area-averaged channels. The obvious solution to this problem is to use a measurement system having a high channel count with many transducers, so that all of the "ordinary" roof taps can be measured simultaneously; the time series obtained can be saved and later reprocessed using appropriate area and modal weighting factors on the required taps. This process can be automated so that a large number of structural members and their natural modes can be examined, without the guesswork involved in a more limited investigation. This is important since, as noted above, it is not obvious which members, modes, and wind directions may result in a critical loading condition. Unless tube lengths are very short, sophisticated digital filtering is usually required to obtain adequate frequency response. Fortunately, such systems have become available and economically feasible

during the past 1-2 years, greatly expanding the application of this technique, in terms of economy, timeliness, and accuracy, to structures of increasing complexity.

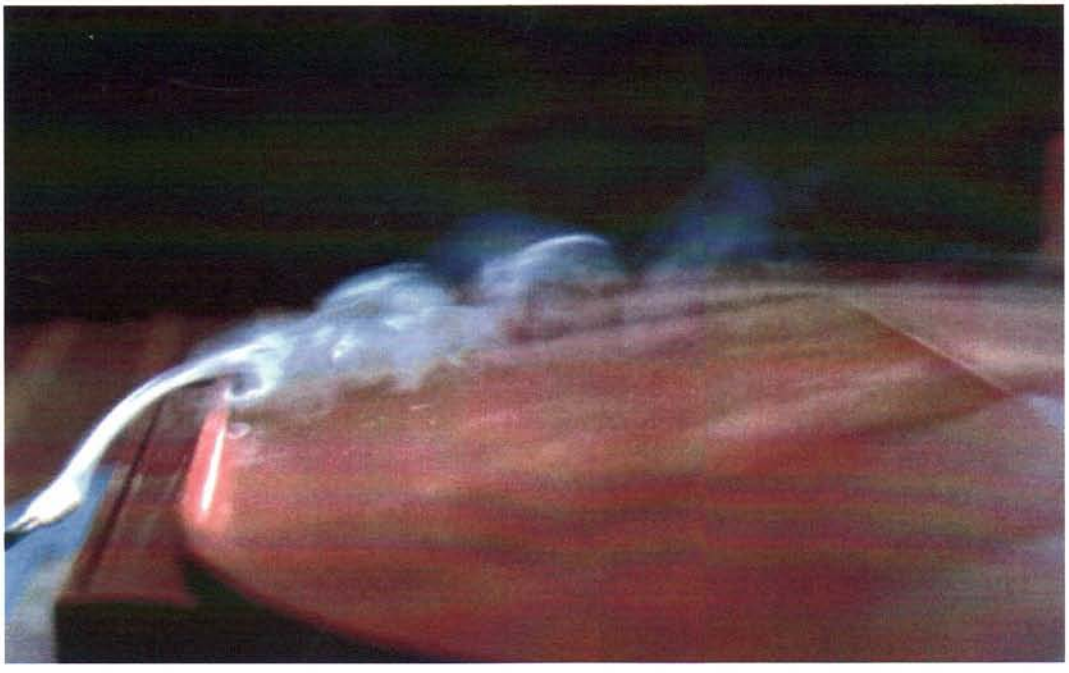

Fig. 1 Visualization of flow due to south wind over Member A, Arena 1

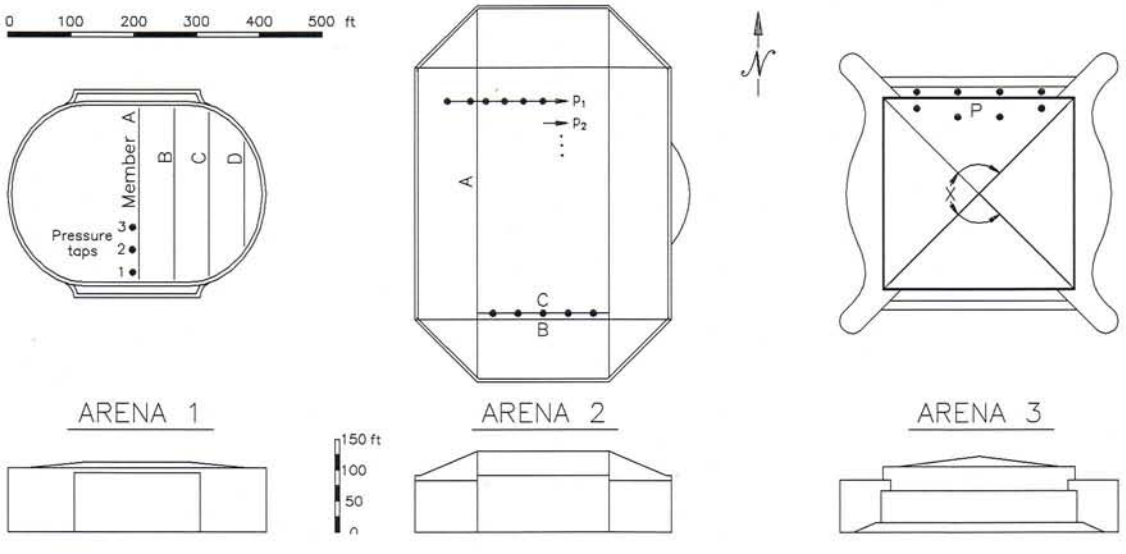

Fig. 2 Example arenas

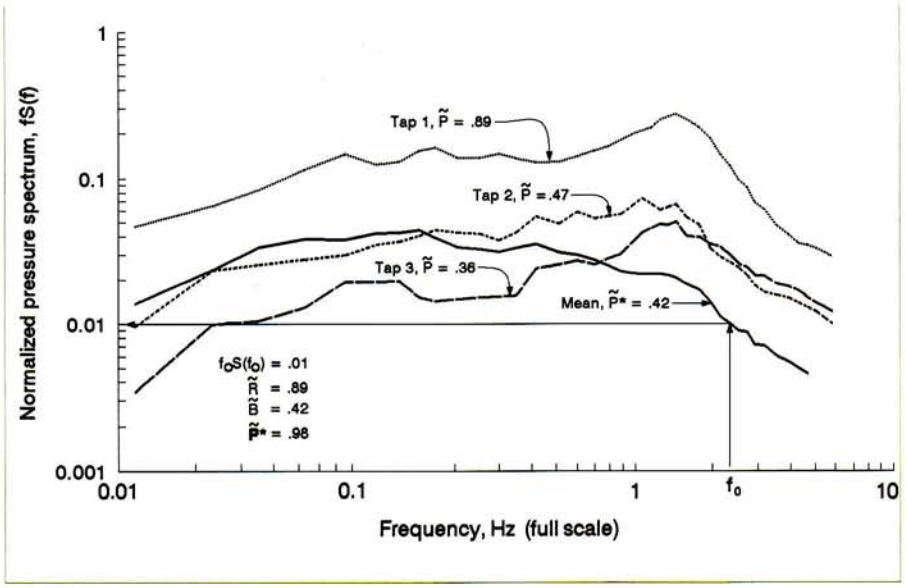

Fig. 3 PSD of pressure at taps on Arena 1

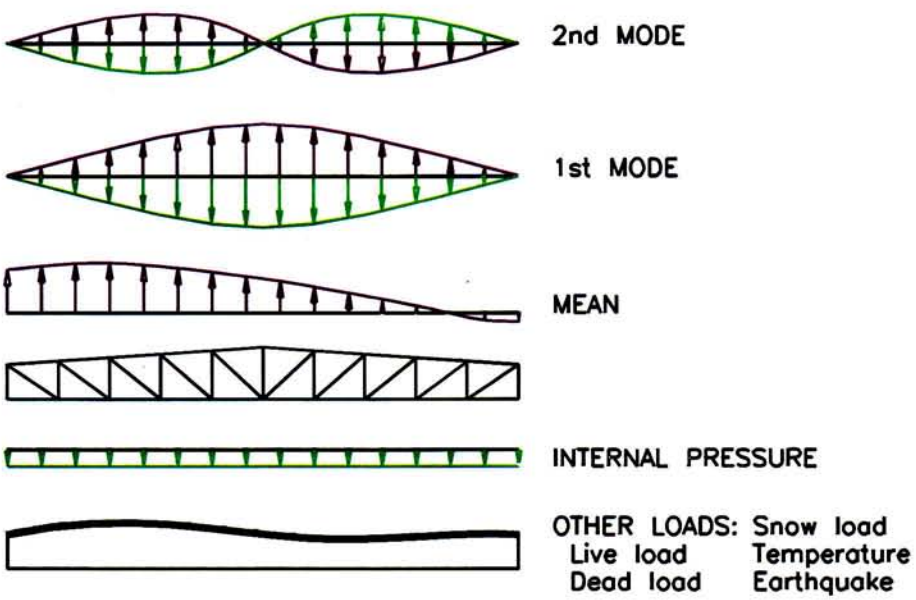

Fig. 4 Illustrative distributions of static-equivalent pressure on a structural member

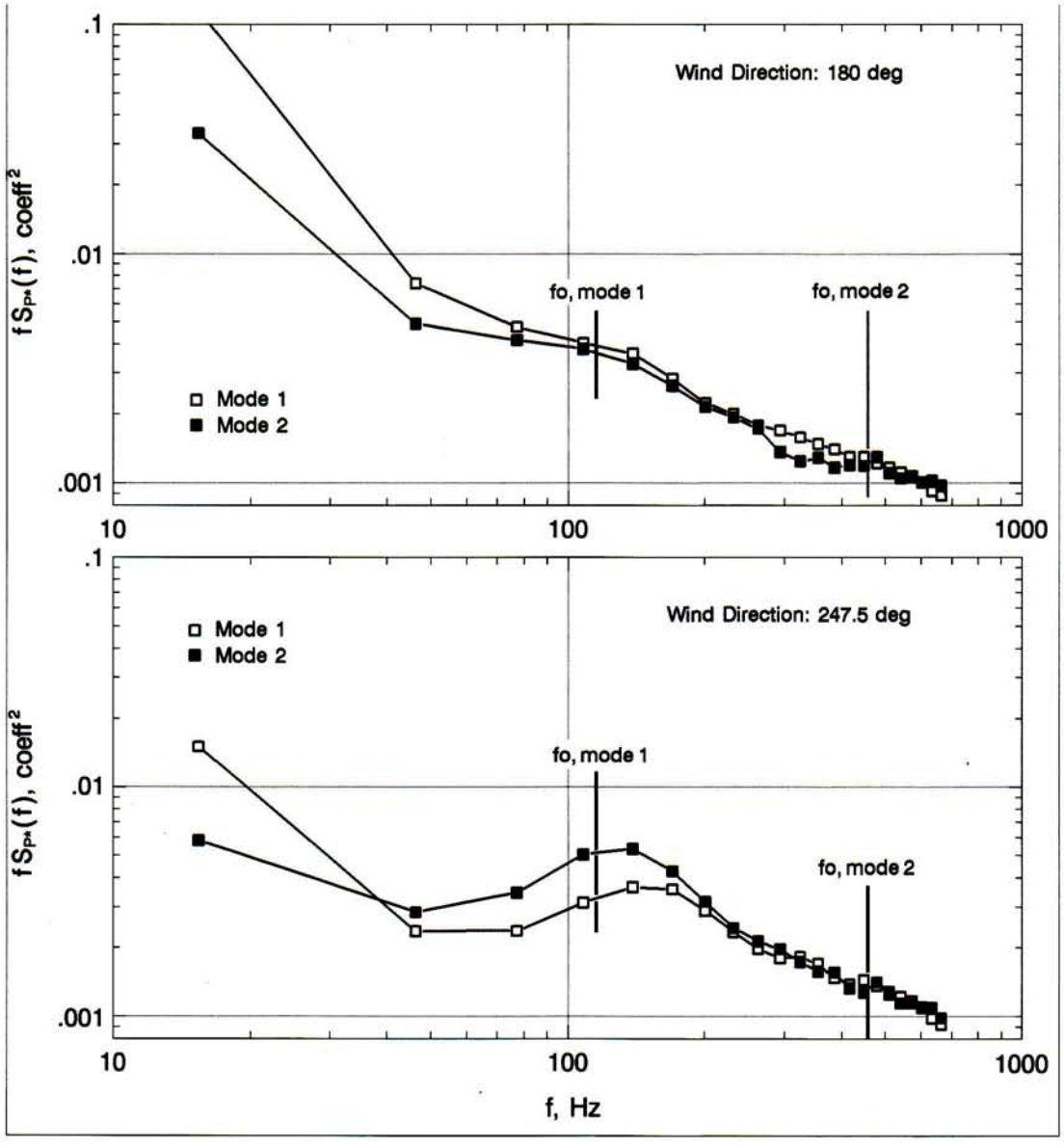

Fig. 5 PSD of generalized load on Member C, Arena 2

Table 1—Wind Loads on Arena No. 1 Members

Truss	Wind Dir.	Wind Tunnel (psf)			ASCE 7-88 Peak (psf)	WT/ ASCE
		Mean	Pk fluct.	Peak		
A	180	-12	±9	-21,-3	-31	0.68
D	90	-24	±15	-40,-9	-25	1.57
D	270	+3	±6	-3,+9	-22	-0.4

Note: Loads are calculated for a fictitious location

Table 2—Nat. Freq. of Major Structural

Arena No.	Member	Mode	f_0, Hz Prot.	Freq. Ratio	f_0, Hz Model
1	A	1	2.25	50	113
	B,C	1	1.9	50	95
	D	1	2.8	50	140
2	A	1	0.7	70	49
		2	1.3	70	91
	B	1	2.45	70	172
		2	3.79	70	265
	C	1	1.65	70	116
		2	6.59	70	461
3	P	1	2.03	60	122
		2	3.82	60	229
	X	1	0.84	60	50
		2,3,4	1.72	60	103